

Original article

Three dimensional anatomical exploration of the anterior hard palate at the level of the third ruga for the placement of mini-implants – a cone-beam CT study

Jan Hourfar^{*,**†}, Georgios Kanavakis^{***†}, Dirk Bister^{****},
Marc Schätzle^{*****}, Layla Awad^{*****}, Manuel Nienkemper^{*****},
Christine Goldbecher^{*****} and Björn Ludwig^{*****}

*Private Practice, Reinheim, Germany, **Department of Orthodontics, University of Heidelberg, Germany, ***Department of Orthodontics, Tufts University School of Dental Medicine, Boston, MA, USA, ****Department of Orthodontics, Guy's and St Thomas' NHS Foundation Trust, London, UK, *****Clinic of Orthodontics and Pediatric Dentistry, Center of Dental Medicine, Zurich, Switzerland, *****Department of Orthodontics, University of Homburg/Saar, Saarland, Germany, *****Department of Orthodontics, Heinrich-Heine-University, Düsseldorf, Germany, *****Private Practice, Halle, Germany, *****Private Practice, Traben-Trarbach, Germany

[†]These authors contributed equally to this article.

Correspondence to: Georgios Kanavakis, Department of Orthodontics and Dentofacial Orthopedics, Tufts University School of Dental Medicine, 1 Kneeland Street, DHS #1145, Boston, MA 02111, USA. E-mail: georgios.kanavakis@tufts.edu; gkanavak@gmail.com

Summary

Aim: The aim of this retrospective investigation was to measure vertical bone thickness on the hard palate, determine areas with adequate bone for the insertion of orthodontic mini-implants (MIs), and provide clinical guidelines for identification of those areas.

Materials and methods: Pre-treatment records of 1007 patients were reviewed by a single examiner. A total of 125 records fulfilled the inclusion criteria and were further investigated. Bone measurements were performed on cone-beam computed tomography scans, at a 90° angle to the bone surface, on 28 predetermined and standardized points on the hard palate. Bone thickness at various areas was associated to clinically identifiable areas on the hard palate by means of pre-treatment plaster models.

Results: Bone thickness ranged between 1.51 and 13.86 mm (total thickness) and 0.33 and 1.65 mm (cortical bone thickness), respectively. Bone thickness was highest in the anterior palate and decreased significantly towards more posterior areas. Plaster model analysis revealed that bone thickness was highest at the level of the third palatal ruga.

Conclusions: The areas on the anterior palate with adequate bone thickness for successful insertion of orthodontic MI correspond to the region of the third palatal ruga. These results provide stable and clinically identifiable landmarks for the insertion of palatal MIs.

Introduction

The use of mini-implants (MIs) in orthodontics has been popularized, primarily due to the possibilities they provide in decreasing or eliminating anchorage loss during orthodontic tooth movements

(1–3). In addition, their small dimensions, the ease of insertion and removal, as well as their relatively small cost in comparison to regular dental implants are further factors constituting them as an effective tool in the orthodontic practice (4).

However, all clinical possibilities created by the use of skeletal anchorage are diminished if the MIs do not remain stable during treatment. The most important factors associated with stability of MIs are cortical bone thickness (5, 6), insertion torque values (5, 7), and root contact (8, 9). Insertion of orthodontic MIs through the buccal attached gingiva into the interradicular space is associated with more risks and higher failure rates, primarily due to greater likelihood of root injury and because cortical bone thickness is less than ideal in most available areas (10, 11).

In order to avoid potential implant failure due to the above-mentioned reasons, MIs can alternatively be placed palatally, in the paramedian area of the anterior maxilla (12). This location can be selected both in adults as well as young patients whose palatal suture has yet not ossified (13). Palatal insertion of MIs offers several advantages such as easy accessibility, minor risk of injuring any anatomical structures, very favourable mucosal tissues as well as sufficient bone (11). However, there is no obvious anatomical structure that can be used as a reference to guide clinicians when placing MIs in the palatal tissues of the anterior maxilla.

In previous studies that utilized computed tomography (CT) imaging in order to assess the quality and quantity of bone in this region, the incisal foramen was selected as an anatomical reference (12, 14–23). However, it is not easy to accurately identify the foramen visually and therefore it cannot be used routinely by clinicians as a landmark. In a CT investigation by Baumgaertel, interproximal tooth contacts were used as reference points to explore the bone of the anterior palate (24). Despite the ease of identifying them as landmarks, occlusal-lingual contact points between teeth are highly variable and their location is greatly influenced by tooth morphology and tooth movements. Therefore, interproximal contacts can also not be considered as clinically stable reference points.

Previous research has proposed that the palatal rugae remain stable with time and can therefore be used as reference points during orthodontic treatment (25). Moreover, various studies investigating longitudinal changes in tooth positions have used the palatal rugae as a reference to superimpose consecutive study models (26–28). Christou and Kiliaridis superimposed the median palatal contour of dental casts, taken at different time points, on the corresponding cephalometric X-rays and found that the third palatal ruga remains particularly stable over time (29). Therefore, one could assume that the area of the third palatal ruga could be a stable landmark to guide the clinician when placing MIs in the anterior palate.

The aim of this investigation was to evaluate bone dimensions in the anterior hard palate using cone-beam CT (CBCT) and to determine appropriate sites for orthodontic MI insertion based on clinically identifiable and stable anatomical landmarks.

Materials and methods

Study population

In order to obtain the sample population, all pre-treatment records from a combined orthodontic/oral surgery clinic in Halle/Saale, Germany were de-identified and reviewed by a single examiner (JH). Permission to review de-identified patient records for the purpose of this study was granted by the local ethics committee (Saarbrücken Ethics Committee, Nr. 221/14).

In order to be included in the study, subjects had to fulfil the following inclusion criteria:

1. Pre-treatment records including plaster models and a large field of view CBCT image of the head. Due to the combined nature of the practice (orthodontics and oral surgery), pre-treatment

CBCT images were also acquired for a variety of reasons, including third molar extractions, exposure of impacted teeth, dental implant placement, etc.

2. No history of previous orthodontic treatment.
3. To ensure comparable dental and skeletal anatomic features of the maxillary dentition and anterior palate, all subjects were of Caucasian origin and had a complete permanent dentition, excluding third molars.

The initial search generated 1007 pre-treatment records. After applying the inclusion criteria, 125 pre-treatment orthodontic records were included in the final sample population. All pre-treatment CBCT images were taken using a Veraviewpocs 3D unit (J. Morita Corp., Osaka, Japan), with a large (15 cm) field of view, at 5 mA and 80 kV. The resulting voxel size was 0.125 mm³ and the slice thickness of the images was 0.25 mm. For all patients, the image was obtained with the head oriented so that the occlusal plane was parallel to the sagittal and transverse planes. In addition, the head was fixed in order to minimize movement artefacts in the final image, and a bite block was used stabilize mandibular position during image acquisition.

Methodology

Description of the measuring matrix

In order to specify and standardize the measuring points on the palate, a measuring grid was created on the palate as displayed on coronal view. The grid consisted of 28 points in total, 12 on the left, 12 on the right of the median palatal suture, and 4 points along the suture (Figure 1). The sagittal reference lines of the grid that are running parallel to the midpalatal suture were based on the contact points between the maxillary central incisors (line '0'), between the central incisor and the lateral incisor (line '1'), and between the lateral incisor and the maxillary canine (line '2').

Measurements along line '0' were performed at a distance of 2 mm from the midpalatal suture due to significant anatomic variation of the suture.

For measurements along the midpalatal suture (s), no reference line was created. Measuring points (s) were defined as the cross-section of the transverse lines to the suture.

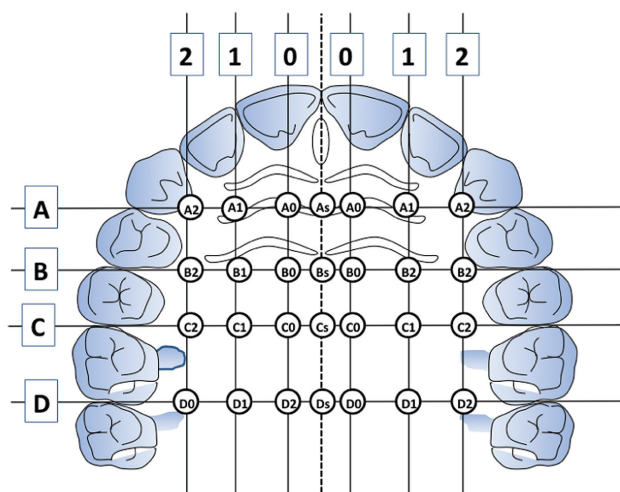


Figure 1. Measuring grid. Bone thickness was measured on the CBCT images, at the 28 points on the grid.

Transverse reference lines were created perpendicular to the sagittal lines, through the contact points between the maxillary canine and first premolar (line 'A'), between the first premolar and second premolar (line 'B'), between the second premolar and first molar (line 'C'), and between the first molar and second molar (line 'D'). All bone measurements were performed at the intersection points of the above-mentioned lines. Intersection points were described with alphanumeric symbols (e.g. A0, As, B1, C2, D4 etc), as displayed in Figure 1.

Digital measurements on 3D images

All measurements were performed using a DICOM imaging software (Osirix®, Version 2.0.1, 64 Bit, Pixmeo, Bernex, Switzerland) for MacOS (Apple, Cupertino, California, USA). After screening of the respective 3D-data sets, orthoradial adjustment according to the x -, y -, and z -plane level was made to enable reproducible 3D measurements. With the use of the described grid, the 28 specific measuring sites were accurately located. Total bone thickness and thickness of the cortical bone were then measured in a split view, at a 90° angle to the bone surface on each site (Figure 2). Along the midpalatal suture, due to the bilateral cortical lining, only one measurement of total bone thickness was performed.

Measurements on plaster models

Plaster models of the maxillary dentition were oriented with the occlusal plane parallel to the horizontal plane. A standardized picture of the maxillary arch was then taken with a digital camera (Canon EOS 450D, Canon Inc., Tokyo, Japan), which was fixed on a tripod at a stable distance from the plaster models, at a 90° angle to the occlusal surface.

On the photographs, perpendicular lines to the mid palatal suture were drawn from the interproximal contacts between the first and second premolars on both sides, and from the most medial end of the third palatal ruga. Then the distance between line 'B' and the third palatal ruga was measured on each side. When line 'B' was located posteriorly to the third palatal ruga, a negative value was recorded for the distance; when it was anteriorly, a positive value was recorded (Figure 3).

Statistical analysis

In order to assess intra-examiner reliability, 40 randomly selected CBCT data sets and plaster models were measured a second time by the same examiner (JH), approximately 1 month after the first

time. The Bland-Altman plots demonstrated a reasonable range of agreement.

The distribution of data was tested by means of the Kolmogorov-Smirnov test and normality of data was not verified. Therefore, comparisons between the right and left sides were performed with the Wilcoxon test for non-parametric data. All analyses were done at the 0.05 level of statistical significance and adjusted accordingly using the Bonferroni correction. No statistically significant differences were found between measurements on the right and left sides, and thus all measurements were pooled together for all subsequent analyses.

Descriptive statistics [medians (Md) and interquartile ranges (IQR)] are presented for bone dimensions at all predetermined points on the measuring grid.

Results

Descriptive results for bone measurements are exhibited in Table 1, as well as Figures 4 and 5.

Total bone thickness

When bone thickness was measured along line '0' in an anteroposterior direction, it was revealed that there were 9.74 mm of bone at point A0 (IQR = 4.29). This was almost twice as much as the amount of bone measured at more posterior points along the line paramedian to the palatal suture (Table 1 and Figure 4).

Along reference line '1', bone thickness was higher at level 'A' (Md = 11.72 mm; IQR = 4.44 mm). Similarly, to the previous results, bone thickness was reduced as measurements were performed at more posterior points along line '1' (i.e. points B1, C1, and D1).

Vertical bone thickness along line '2' also exhibited the highest values at points 'A2' on the measuring grid (Md = 13.86 mm; IQR = 5.06 mm) and a significant reduction of bone thickness at more posterior points (i.e. B2, C2, and D2).

Finally, midpalatal bone thickness(s) presented the same trend in bone thickness. Highest values were measured anteriorly

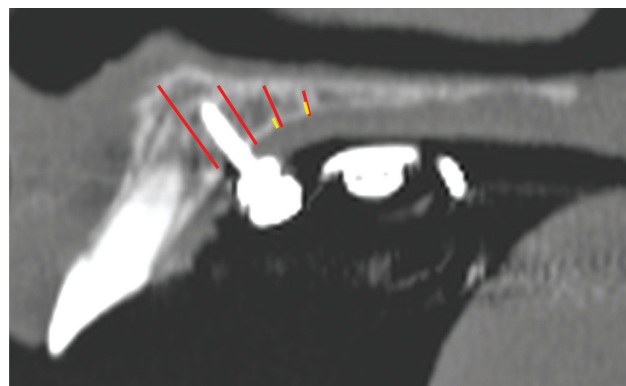


Figure 2. Measurements of total bone thickness (red line) and cortical bone thickness (yellow line) were performed at the same points.

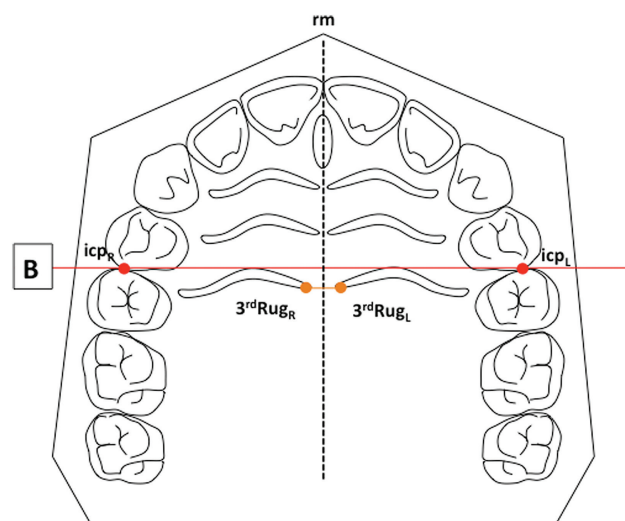


Figure 3. Measurements on plaster models. Perpendicular lines were dropped from the contact point between the first and second maxillary premolars on the palatal midline (suture). The distance between the median end of the third ruga and line(s) 'B' was measured on each side separately. A positive value was recorded when line 'B' was located anteriorly to the median end of the third ruga.

Table 1. Total bone thickness and cortical bone thickness at various points on the measuring grid.

		Transverse reference lines			
		s	0	1	2
Total bone thickness (median/IQR)					
Anterior–posterior reference lines	A	12.27 (2.14)	9.74 (4.29)	11.72 (4.44)	13.86 (5.06)
	B	6.59 (2.64)	4.62 (2.64)	4.50 (3.39)	6.65 (5.04)
	C	4.66 (1.67)	2.89 (2.25)	2.39 (1.97)	4.09 (2.64)
	D	4.53 (1.60)	3.10 (1.96)	1.51 (1.24)	2.72 (1.73)
Cortical bone thickness (median/IQR)					
Anterior–posterior reference lines	A	—	1.40 (0.49)	1.49 (0.50)	1.65 (0.58)
	B	—	0.83 (0.33)	0.78 (0.41)	1.08 (0.57)
	C	—	0.58 (0.33)	0.50 (0.33)	0.68 (0.51)
	D	—	0.58 (0.33)	0.33 (0.20)	0.41 (0.25)

IQR, interquartile range.

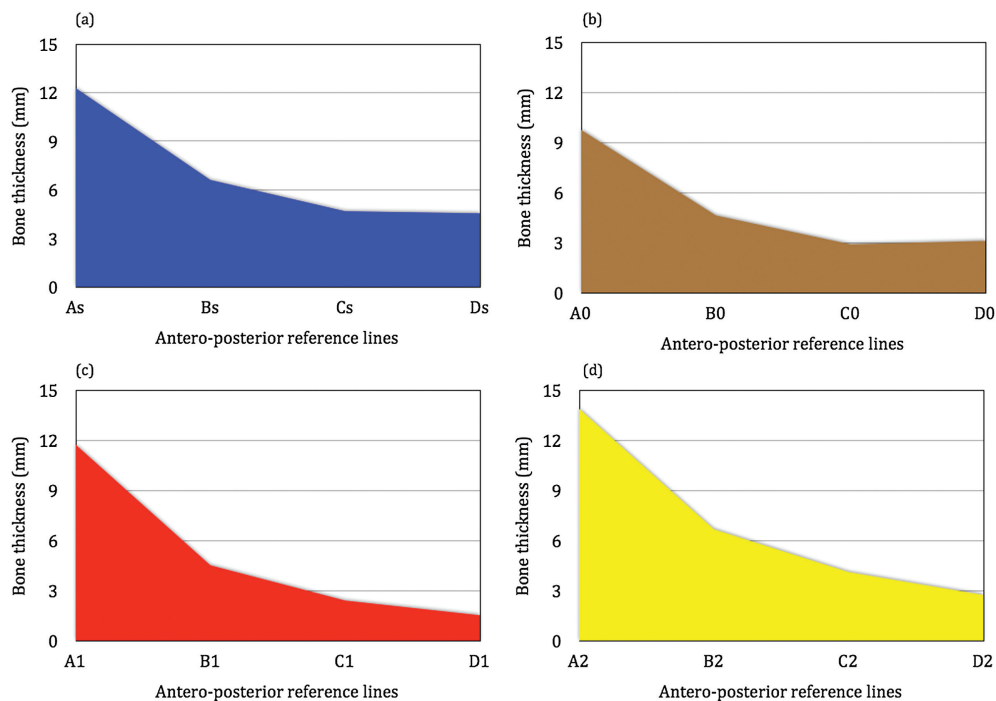


Figure 4. Total bone thickness midpalatally (a) and along reference lines '0' (b), '1' (c), and '2' (d).

($Md_{As} = 12.27$ mm; $IQR_{As} = 2.14$ mm) at point As and were reduced more posteriorly (Table 1 and Figure 4).

Cortical bone thickness

Cortical bone thickness was highest at level 'A' along all three lines of measurement (i.e. lines '1', '2', and '3') with values ranging between 1.40 (point 'A0') and 1.65 (point 'A2') mm. At more posterior points (levels 'B–D'), cortical bone thickness was significantly reduced (Table 1 and Figure 5). A considerable dispersion of values was evident between measurements at various points on the grid.

Measurements along lines 'A' and 'B'

According to the measurements performed on the plaster models, line 'B' was located approximately 0.8 mm on average ($M = 0.77$; $SD = 1.44$) posteriorly to the median ends of the third palatal ruga.

Measuring points along lines 'A' and 'B' exhibited the highest values in total and cortical bone thickness compared to all other

measuring points on the grid. Values of total bone thickness ranged between 4.62 mm at 'B0' and 13.86 mm at 'A2', and cortical bone thickness ranged between 0.83 mm at 'B0' and 1.65 mm at 'A2'.

Discussion

The aim of this descriptive anatomical investigation was to evaluate total and cortical bone availability of the hard palate for the insertion of orthodontic MIs. For this purpose, a measuring grid was used, based on clinically reproducible dental contact points.

Based on the results, the largest amount of bone in the hard palate is found along line 'A', which runs between the contact points of the right and left maxillary canines and first premolars. Bone height at points 'As', 'A0', 'A1', and 'A2' ranged between 9.74 and 13.86 mm. These results are in agreement with previous anatomical investigations that have also revealed significantly more bone in the anterior section, compared to other areas of the hard palate (24). Stockmann *et al.* (30) specifically reported that the most bone in the

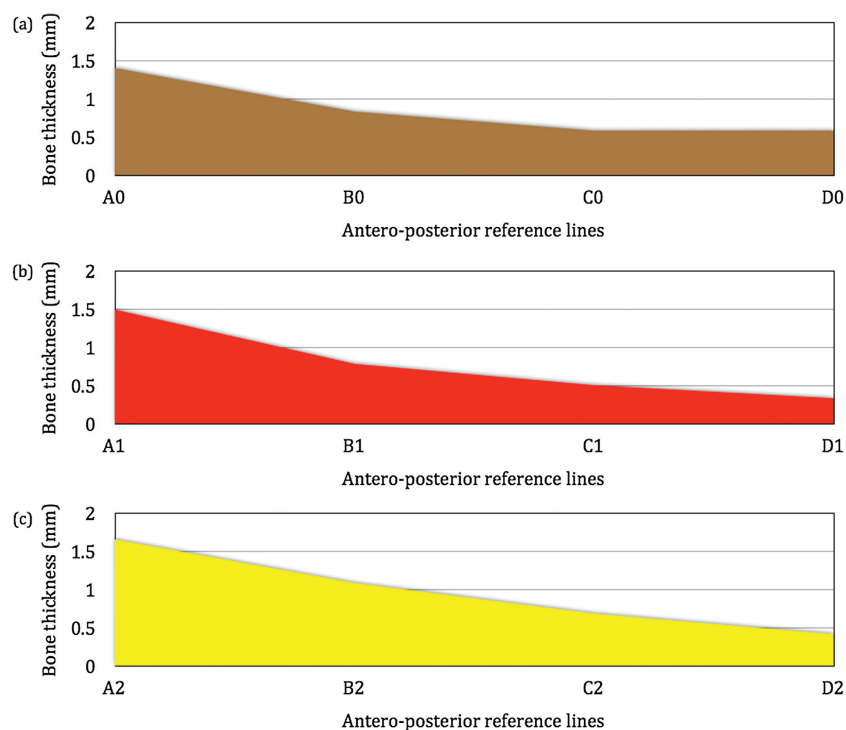


Figure 5. Cortical bone thickness along reference lines '0' (a), '1' (b), and '2' (c).

palate was found at the level of the first premolar, which is in close proximity to line 'A' in the grid that was used for our study.

Measurements of the cortical bone height further supported the superiority of the anterior palate for the placement of orthodontic implants. According to previous research, cortical bone thickness is vital for the success of orthodontic MIs (31) and studies evaluating the critical factors for initial stability have concluded that at least 1 mm of cortical bone is required (5). In this investigation, cortical bone thickness ranged between 1.40 and 1.65 mm along line 'A' and appeared to be slightly increased closer to the lateral borders of the palate. More posteriorly, at point 'B2', cortical bone was also adequate with a median thickness of 1.08 mm. However, at more posterior points, cortical bone thickness was found to be less than 1 mm on average.

In cases requiring insertion of MIs in more posterior areas of the hard palate, the midpalatal suture might thus be a preferred option. Due to bilateral cortical lining at the suture, total bony support for MIs is adequate for good stability (Table 1 and Figure 4). Nienkemper *et al.* (32) compared the stability between paramedian and median implant placement and were not able to find significant long-term differences after the first 4 weeks from the day of placement. Furthermore, midpalatal MI placement has exhibited good clinical success and is recommended for the fabrication of various fixed orthodontic appliances (33, 34).

Earlier radiographic studies had suggested that the palatal area between the second and first molars as well as between the second premolar and first molar would be 'safe zones' for the insertion of orthodontic MIs, as long as the distance from the alveolar crest was adequate (35). These areas correspond to points 'C1', 'C2', 'D1', and 'D2' on our measuring grid, where cortical bone was significantly less than 1 mm. Thus, based on the results of this study, in the posterior palatal interradicular areas, there is not enough cortical bone to provide good primary stability.

More recent CBCT studies have produced similar results to the present ones and have demonstrated that palatal bone dimensions

decrease significantly towards more posterior areas of the palate (12, 14, 18). The midpalatal suture might be an exception to this rule, with bone thickness increasing posteriorly (14); however, this was not confirmed by our findings, and midpalatal bone height was also found to be higher in the anterior hard palate. Similarly, Moon *et al.* (36) reported that bone density was highest within 3 mm around the midpalatal suture and tended to decrease towards more posterior areas of the palate.

Unfortunately, direct comparisons between studies exploring palatal bone thickness are not always possible because of differences in methodologies. While some researchers used clinically identifiable dental coordinates, such as contact points (24), as reference structures, other preferred to use radiographic anatomical structures such as the incisive foramen (12, 14, 16–18). There are advantages and disadvantages to both methods. Although the incisive foramen is a stable anatomical structure and thus provides a reliable anatomical reference, it cannot be identified clinically (11). On the other hand, using dental contact points as reference structures provides a good clinical guide for implant placement; nevertheless the reliability of the method is questionable. In cases with severe crowding or tooth migration, which are common in orthodontic patients, the value of the method is restricted.

The present investigation introduced the median end of the most distal palatal ruga as a clinically identifiable and anatomically stable landmark. Previous research proposed that the palatal rugae remain stable over time and can therefore be used as reference points during orthodontic treatment (25). Moreover, numerous studies investigating longitudinal changes in tooth positions have used the palatal rugae as a reference to superimpose consecutive study models (26–28).

Superimposition of the plaster models on the CBCT images revealed that line 'B' was located less than 1 mm on average posteriorly to the median ends of the third palatal ruga. In addition, according to our results, all points along line 'A' on the

measuring grid, as well as point 'B2' exhibited adequate bone thickness to provide good primary implant stability. It can thus be concluded that the area around the third palatal ruga not only is a stable and clinically identifiable anatomical landmark, but also provides superior bone thickness for the placement of orthodontic MIs.

The validity and accuracy of measurements performed with Osirix® software, which was used in this investigation, have been demonstrated by various previous studies (37–42). Kim *et al.* (43) evaluated the accuracy and precision of Osirix® for linear measurements in 3D datasets and found no significant differences compared to measurements performed with a digital caliper. This finding is also supported by Yamauchi *et al.* (44), who compared Osirix® to other commercial software and reported equivalent results.

The present morphological exploration of the hard palate by means of CBCT imaging provides clinical guidelines for the placement of orthodontic MIs. The area around the third palatal ruga exhibited the highest values of bone thickness. In more posterior areas, bone availability decreases significantly and therefore achieving stability of MIs might not always be possible, unless sutural insertion is selected. Nevertheless, in areas where bone is limited, selecting a longer MI might engage the cortical bone the nasal cavity floor, thus providing bicortical anchorage, which significantly increases the stability of skeletal anchorage devices (45). Although in some cases penetration into the nasal cavity may occur, complications are unlikely to occur (46, 47).

Our results should not be interpreted in isolation, but in combination with previous studies. In patients with severely proclined incisors, there is an increased possibility of root injury, if the path of implant insertion is not carefully planned. At the level of the third palatal ruga, however, an oblique path of insertion significantly reduces the risk of injury, if a 6 or 8 mm long MI is used (48). Moreover, when implant placement in the anterior palate is challenging—due to a deep palatal vault, for example—and a more posterior insertion site is required, the midpalatal suture becomes the insertion site of choice.

The findings of the present investigation further improve our knowledge regarding palatal bone thickness in relation to clinically identifiable and anatomically stable landmarks (i.e. palatal rugae). These new clinical guidelines may minimize the need for radiographic imaging prior to the insertion of orthodontic MIs.

Conclusions

1. Palatal bone thickness is increased in the anterior hard palate, at the level of the third palatal ruga.
2. Bone availability significantly reduces in most posterior areas of the hard palate.
3. The third palatal ruga provides a stable and clinically identifiable landmark for the insertion of orthodontic MIs.

Acknowledgement

The authors would like to thank Dr Heiko Goldbecher for providing the identified pool of patient records.

References

1. Creekmore, T.D. and Eklund, M.K. (1983) The possibility of skeletal anchorage. *Journal of Clinical Orthodontics*, 17, 266–269.
2. Papadopoulos, M.A., Papageorgiou, S.N. and Zogakis, I.P. (2011) Clinical effectiveness of orthodontic miniscrew implants: a meta-analysis. *Journal of Dental Research*, 90, 969–976.
3. Kanomi, R. (1997) Mini-implant for orthodontic anchorage. *Journal of Clinical Orthodontics*, 31, 763–767.
4. Papadopoulos, M.A. and Tarawneh, F. (2007) The use of miniscrew implants for temporary skeletal anchorage in orthodontics: a comprehensive review. *Oral Surgery, Oral Medicine, Oral Pathology, Oral Radiology, and Endodontology*, 103, 6–15.
5. Motoyoshi, M., Yoshida, T., Ono, A. and Shimizu, N. (2007) Effect of cortical bone thickness and implant placement torque on stability of orthodontic mini-implants. *International Journal of Oral and Maxillofacial Implants*, 22, 779–784.
6. Motoyoshi, M., Inaba, M., Ono, A., Ueno, S. and Shimizu, N. (2009) The effect of cortical bone thickness on the stability of orthodontic mini-implants and on the stress distribution in surrounding bone. *International Journal of Oral and Maxillofacial Surgery*, 38, 13–18.
7. Motoyoshi, M., Hirabayashi, M., Uemura, M. and Shimizu, N. (2006) Recommended placement torque when tightening an orthodontic mini-implant. *Clinical Oral Implants Research*, 17, 109–114.
8. Kang, Y.G., Kim, J.Y., Lee, Y.J., Chung, K.R. and Park, Y.G. (2009) Stability of mini-screws invading the dental roots and their impact on the parodontal tissues in beagles. *Angle Orthodontist*, 79, 248–255.
9. Chen, Y.H., Chang, H.H., Chen, Y.J., Lee, D., Chiang, H.H. and Yao, C.C. (2008) Root contact during insertion of miniscrews for orthodontic anchorage increases the failure rate: an animal study. *Clinical Oral Implants Research*, 19, 99–106.
10. Kravitz, N.D. and Kusnoto, B. (2007) Risks and complications of orthodontic miniscrews. *American Journal of Orthodontics and Dentofacial Orthopedics*, 131, S43–S51.
11. Ludwig, B., Glasl, B., Bowman, S.J., Wilmes, B., Kinzinger, G.S. and Lisson, J.A. (2011) Anatomical guidelines for miniscrew insertion: palatal sites. *Journal of Clinical Orthodontics*, 45, 433–441.
12. King, K.S., Lam, E.W., Faulkner, M.G., Heo, G. and Major, P.W. (2007) Vertical bone volume in the paramedian palate of adolescents: a computed tomography study. *American Journal of Orthodontics and Dentofacial Orthopedics*, 132, 783–788.
13. Karagiolidou, A., Ludwig, B., Pazera, P., Gkantidis, N., Pandis, N. and Katsaros, C. (2013) Survival of palatal miniscrews used for orthodontic appliance anchorage: a retrospective cohort study. *American Journal of Orthodontics and Dentofacial Orthopedics*, 143, 767–772.
14. Ryu, J.H., Park, J.H., Vu Thi Thu, T., Bayome, M., Kim, Y. and Kook, Y.A. (2012) Palatal bone thickness compared with cone-beam computed tomography in adolescents and adults for mini-implant placement. *American Journal of Orthodontics and Dentofacial Orthopedics*, 142, 207–212.
15. Gracco, A., Lombardo, L., Cozzani, M. and Siciliani, G. (2006) Quantitative evaluation with CBCT of palatal bone thickness in growing patients. *Progress in Orthodontics*, 7, 164–174.
16. Gracco, A., Lombardo, L., Cozzani, M. and Siciliani, G. (2008) Quantitative cone-beam computed tomography evaluation of palatal bone thickness for orthodontic miniscrew placement. *American Journal of Orthodontics and Dentofacial Orthopedics*, 134, 361–369.
17. Gracco, A., Luca, L., Cozzani, M. and Siciliani, G. (2007) Assessment of palatal bone thickness in adults with cone beam computerised tomography. *Australian Orthodontic Journal*, 23, 109–113.
18. Kang, S., Lee, S.J., Ahn, S.J., Heo, M.S. and Kim, T.W. (2007) Bone thickness of the palate for orthodontic mini-implant anchorage in adults. *American Journal of Orthodontics and Dentofacial Orthopedics*, 131, S74–S81.
19. Farnsworth, D., Rossouw, P.E., Ceen, R.F. and Buschang, P.H. (2011) Cortical bone thickness at common miniscrew implant placement sites. *American Journal of Orthodontics and Dentofacial Orthopedics*, 139, 495–503.
20. Bernhart, T., Vollgruber, A., Gahleitner, A., Dörtbudak, O. and Haas, R. (2000) Alternative to the median region of the palate for placement of an orthodontic implant. *Clinical Oral Implants Research*, 11, 595–601.
21. Gahleitner, A., Podesser, B., Schick, S., Watzek, G. and Imhof, H. (2004) Dental CT and orthodontic implants: imaging technique and assessment

- of available bone volume in the hard palate. *European Journal of Radiology*, 51, 257–262.
22. King, K.S., Lam, E.W., Faulkner, M.G., Heo, G. and Major, P.W. (2006) Predictive Factors of Vertical Bone Depth in the Paramedian Palate of Adolescents. *Angle Orthodontist*, 76, 745–751.
 23. Jayakumar, G., Rajkumar, B.T., George, M.A. and Krishnaswamy, N.R. (2012) Quantitative assessment of palatal bone thickness in an ethnic Indian population: a computed tomography study. *Indian Journal of Dental Research*, 23, 49–52.
 24. Baumgaertel, S. (2009) Quantitative investigation of palatal bone depth and cortical bone thickness for mini-implant placement in adults. *American Journal of Orthodontics and Dentofacial Orthopedics*, 136, 104–108.
 25. Kim, H.K., Moon, S.C., Lee, S.J. and Park, Y.S. (2012) Three-dimensional biometric study of palatine rugae in children with a mixed-model analysis: a 9-year longitudinal study. *American Journal of Orthodontics and Dentofacial Orthopedics*, 141, 590–597.
 26. Hoggan, B.R. and Sadowsky, C. (2001) The use of palatal rugae for the assessment of anteroposterior tooth movements. *American Journal of Orthodontics and Dentofacial Orthopedics*, 119, 482–488.
 27. Almeida, M.A., Phillips, C., Kula, K. and Tulloch, C. (1995) Stability of the palatal rugae as landmarks for analysis of dental casts. *Angle Orthodontist*, 65, 43–48.
 28. Bailey, L.T.J., Esmailnejad, A. and Almeida, M.A. (1996) Stability of the palatal rugae as landmarks for analysis of dental casts in extraction and nonextraction cases. *Angle Orthodontist*, 66, 73–78.
 29. Christou, P. and Kiliaridis, S. (2008) Vertical growth-related changes in the positions of palatal rugae and maxillary incisors. *American Journal of Orthodontics and Dentofacial Orthopedics*, 133, 81–86.
 30. Stockmann, P., Schlegel, K.A., Srour, S., Neukam, F.W., Fenner, M. and Felszeghy, E. (2009) Which region of the median palate is a suitable location of temporary orthodontic anchorage devices? A histomorphometric study on human cadavers aged 15–20 years. *Clinical Oral Implants Research*, 20, 306–312.
 31. Wilmes, B., Rademacher, C., Olthoff, G., Drescher, D. (2006) Parameters affecting primary stability of orthodontic mini-implants. *Journal of Orofacial Orthopedics*, 67, 162–174.
 32. Nienkemper, M., Pauls, A., Ludwig, B. and Drescher, D. (2013) Stability of paramedian inserted palatal mini-implants at the initial healing period: a controlled clinical study. *Clinical Oral Implants Research*, 27, 12321.
 33. Wilmes, B. and Drescher, D. (2010) Application and effectiveness of the Beneslider: a device to move molars distally. *World Journal of Orthodontics*, 11, 331–340.
 34. Nienkemper, M., Wilmes, B., Pauls, A. and Drescher, D. (2012) Multipurpose use of orthodontic mini-implants to achieve different treatment goals. *Journal of Orofacial Orthopedics*, 73, 467–476.
 35. Poggio, P.M., Incorvati, C., Velo, S. and Carano, A. (2006) “Safe zones”: a guide for miniscrew positioning in the maxillary and mandibular arch. *Angle Orthodontist*, 76, 191–197.
 36. Moon, S.H., Park, S.H., Lim, W.H. and Chun, Y.S. (2010) Palatal bone density in adult subjects: implications for mini-implant placement. *Angle Orthodontist*, 80, 137–144.
 37. Albert, S., Cristofari, J.P., Cox, A., Bensimon, J.L., Guedon, C. and Barry, B. (2011) Mandibular reconstruction with fibula free flap. Experience of virtual reconstruction using Osirix(R), a free and open source software for medical imagery. *Annales de Chirurgie Plastique et Esthetique*, 56, 494–503.
 38. Fortin, M. and Battie, M.C. (2012) Quantitative paraspinal muscle measurements: inter-software reliability and agreement using OsiriX and ImageJ. *Physical Therapy*, 92, 853–864.
 39. Jalbert, F. and Paoli, J.R. (2008) Osirix: free and open-source software for medical imagery. *Revue de Stomatologie et de Chirurgie Maxillo-faciale*, 109, 53–55.
 40. Melissano, G., Bertoglio, L., Civelli, V., Amato, A.C., Coppi, G., Civilini, E., Calori, G., De Cobelli, F., Del Maschio, A. and Chiesa, R. (2009) Demonstration of the Adamkiewicz artery by multidetector computed tomography angiography analysed with the open-source software OsiriX. *European Journal of Vascular and Endovascular Surgery*, 37, 395–400.
 41. Sierra-Martinez, E., Cienfuegos-Monroy, R. and Fernandez-Sobrinho, G. (2009) OsiriX, a useful tool for processing tomographic images in patients with facial fracture. *Cirugia y Cirujanos*, 77, 95–99.
 42. Wang, Y.C., Liu, Y.C., Hsieh, T.C., Lee, S.T. and Li, M.L. (2010) Aneurysmal subarachnoid hemorrhage diagnosis with computed tomographic angiography and OsiriX. *Acta Neurochirurgica*, 152, 263–269.
 43. Kim, G., Jung, H.J., Lee, H.J., Lee, J.S., Koo, S. and Chang, S.H. (2012) Accuracy and Reliability of Length Measurements on Three-Dimensional Computed Tomography Using Open-Source OsiriX Software. *Journal of Digital Imaging*, 25, 486–491.
 44. Yamauchi, T., Yamazaki, M., Okawa, A., Furuya, T., Hayashi, K., Sakuma, T., Takahashi, H., Yanagawa, N. and Koda M. (2010) Efficacy and reliability of highly functional open source DICOM software (OsiriX) in spine surgery. *Journal of Clinical Neuroscience*, 17, 756–759.
 45. Brettin, B.T., Grosland, N.M., Qian, F., Southard, K.A., Stuntz, T.D., Morgan, T.A., Marshall, S.D. and Southard, T.E. (2008) Bicortical vs monocortical orthodontic skeletal anchorage. *American Journal of Orthodontics and Dentofacial Orthopedics*, 134, 625–635.
 46. Branemark, P.I., Adell, R., Albrektsson, T., Lekholm, U., Lindstrom, J. and Rockler, B. (1984) An experimental and clinical study of osseointegrated implants penetrating the nasal cavity and maxillary sinus. *Journal of Oral and Maxillofacial Surgery*, 42, 497–505.
 47. Greenstein, G., Cavallaro, J., Romanos, G. and Tarnow, D. (2008) Clinical recommendations for avoiding and managing surgical complications associated with implant dentistry: a review. *Journal of Periodontology*, 79, 1317–1329.
 48. Hourfar, J., Ludwig, B., Bister, D., Braun, A. and Kanavakis, G. (2014) The most distal palatal ruga for placement of orthodontic mini-implants. *European Journal of Orthodontics*, 37, 373–378.